

RESEARCH ARTICLE

Bacterial surface display of human lectins in *Escherichia coli*

Alba Vázquez-Arias^{1,2} | Lorena Vázquez-Iglesias^{1,2} | Ignacio Pérez-Juste³ |
 Jorge Pérez-Juste^{1,2,3} | Isabel Pastoriza-Santos^{1,2,3} | Gustavo Bodelon^{1,2,4} 

¹CINBIO, Universidade de Vigo, Vigo, Spain

²Galicia Sur Health Research Institute (IIS Galicia Sur), SERGAS-UVIGO, Vigo, Spain

³Departamento de Química Física, Universidade de Vigo, Vigo, Spain

⁴Departamento de Biología Funcional y Ciencias de la Salud, Universidade de Vigo, Vigo, Spain

Correspondence

Gustavo Bodelon, CINBIO, Universidade de Vigo, 36310 Vigo, Spain.
 Email: gbodelon@uvigo.gal

Funding information

European Regional Development Fund - ERDF; Horizon 2020 Framework Programme, Grant/Award Number: 965018—BIOCELLPHE; Ministerio de Ciencia e Innovación, Grant/Award Number: PID2019-108954RB-I00, PID2019-109669RB-I00 and PID2022-138023NB-I00; Xunta de Galicia (Centro singular de investigación de Galicia accreditation 2019-2022)

Abstract

Lectin-glycan interactions sustain fundamental biological processes involved in development and disease. Owing to their unique sugar-binding properties, lectins have great potential in glycobiology and biomedicine. However, their relatively low affinities and broad specificities pose a significant challenge when used as analytical reagents. New approaches for expression and engineering of lectins are in demand to overcome current limitations. Herein, we report the application of bacterial display for the expression of human galectin-3 and mannose-binding lectin in *Escherichia coli*. The analysis of the cell surface expression and binding activity of the surface-displayed lectins, including point and deletion mutants, in combination with molecular dynamics simulation, demonstrate the robustness and suitability of this approach. Furthermore, the display of functional mannose-binding lectin in the bacterial surface proved the feasibility of this method for disulfide bond-containing lectins. This work establishes for the first time bacterial display as an efficient means for the expression and engineering of human lectins, thereby increasing the available toolbox for glycobiology research.

INTRODUCTION

Glycans are oligosaccharides found in all kingdoms of life covalently linked to proteins, lipids and nucleic acids (Broussard et al., 2019; Flynn et al., 2021). The complete repertoire of glycans and their glycoconjugates is involved in a vast range of cellular functions and key physiological processes including cellular communication, adhesion, proliferation, differentiation, apoptosis, self-recognition and immune response, among many others (Varki, 2017). Not surprisingly, abnormal glycan expression is involved in a wide range of diseases, immune deficiencies, hereditary disorders and many types of cancers (Magalhães et al., 2021; Pinho &

Reis, 2015; Reilly et al., 2019). Glycans also play prominent roles in host-pathogen interactions and immune evasion (Lin et al., 2020; Miller et al., 2021; Zhang & Qu, 2021).

In nature, the staggering molecular information encoded in glycomes is deciphered by carbohydrate-binding lectins. Lectins selectively recognise and reversibly bind to sugars and glycoconjugates in a process mediated by the carbohydrate-recognition domain (CRD) (André et al., 2015; Gabius et al., 2021). To meet the ample spectrum required for glycan recognition, lectins have evolved a large structural diversity that has been divided into 109 classes, 350 families and 35 folds (Bonnardel et al., 2021), including C-type lectins, I-type

This is an open access article under the terms of the [Creative Commons Attribution-NonCommercial](https://creativecommons.org/licenses/by-nc/4.0/) License, which permits use, distribution and reproduction in any medium, provided the original work is properly cited and is not used for commercial purposes.

© 2024 The Authors. *Microbial Biotechnology* published by Applied Microbiology International and John Wiley & Sons Ltd.

lectins, galectin (or S-type), pentraxins and P-type lectins (Raposo et al., 2021). Owing to their unique glycan-binding properties, purified lectins are being extensively investigated as tools for biomedical and biotechnological applications (Chettri et al., 2021; Coelho et al., 2017), including structural characterisation of glycans, cell typing, histology and high-throughput analysis of complex carbohydrates in microarrays (Dang et al., 2020). Despite their enormous potential, the relatively weak binding affinity of individual interactions between lectins and carbohydrates (K_d values in the μM – mM range) has impaired their broad use as analytical reagents. Nature circumvented this limitation through oligomerisation and multivalency, as lectins tend to assemble into oligomeric structures containing multiple binding sites, thus allowing for higher affinities to be reached (Cecioni et al., 2014).

The affinity, stability and/or specificity of carbohydrate-binding proteins can be improved by protein engineering approaches (Hu et al., 2015; Ward et al., 2021; Warkentin & Kwan, 2021). Phage and cell surface display systems are powerful techniques for the engineering and streamlined screening of binders from genetically encoded libraries (Mahdavi et al., 2022). In phage display, the peptides of interest are expressed on the viral surface fused to virion coat proteins so they can interact with targets present in the external milieu. This technique has been successfully used for the selection of peptides, and affinities in the sub-nanomolar range are typically achieved for recombinant antibodies (Jaroszewicz et al., 2022; Mahdavi et al., 2022). However, the small size of the viral particle severely limits the number of copies of the displayed peptide (i.e., valency), which may hamper the selection of binders with intrinsic low affinity such as lectins. Conversely, display in mammalian, yeast and bacterial cells allows the presentation of large peptides and proteins in the cell surface at much higher numbers. For instance, yeast display allows the surface expression of ca. 5×10^4 molecules of single-chain antibody fragments (scFvs) per cell (Salema & Fernández, 2017), whereas fusion to the minor coat pIII protein of filamentous phages can only achieve the display of up to five copies of scFvs per virion (Sartorius et al., 2019). Therefore, although phage display has been exploited for small glycoconjugates and carbohydrate epitopes (Çelik et al., 2010; Sojitra et al., 2021), its application for lectin selection remains to be explored. Mammalian and yeast display allows posttranslational modifications, correct folding and glycosylation of eukaryotic organisms; however, only relatively small size libraries (10^7 – 10^9) can be obtained by these methods (Valldorf et al., 2022). The selection of human lectins by mammalian display is hampered by the existence of endogenous carbohydrate-binding proteins in the cell surface, and the use of yeast for the surface expression of human lectins is yet to be fully developed. In this context, Ryckaert et al. investigated the display

of 6 members of galectins, siglecs and C-type lectin subfamilies on the surface of *Saccharomyces cerevisiae* and *Pichia pastoris*. Among them, only galectin-3 and galectin-1, as well as the sialoadhesin α -agglutinin, presented glycan-binding activities upon expression in *S. cerevisiae* and *P. pastoris*, respectively. The lack of activity observed for some of the lectins assessed in this study was attributed to their low expression levels, as well as incorrect topological orientation of the CRD for carbohydrate binding (Ryckaert et al., 2007). Bacterial display relies on the use of a membrane anchoring motif that promotes the translocation of a heterologous polypeptide across the cellular membrane to the extracellular milieu (Georgiou et al., 1997). Bacterial display in *Escherichia coli* benefits from its high transformation efficiency, stability of the cloned DNA and fast growth. Also, along with multivalent expression, this technology allows the implementation of flow cytometry-based methods for selection and screening of affinity binders (Salema & Fernández, 2017).

In this study, we applied bacterial display for the engineering and cell surface expression of human lectins in *E. coli*. To this end, we investigated a display system based on an adhesin from enteropathogenic and enterohemorrhagic *E. coli* termed intimin (McWilliams et al., 2014; Figure 1A). The N-terminal region of intimin contains a Sec signal peptide, a LysM-type region and a β -barrel domain that spans the outer membrane (OM) (Fairman et al., 2012). The extracellular C-terminal region is comprised of four tandem immunoglobulin-like domains (D00–D0–D1–D2) and a C-type lectin domain (D3) (Batchelor, 2000; Luo et al., 2000; Weikum et al., 2020) that contains a disulfide bridge which may be involved in receptor binding (Bodelón et al., 2009; Frankel et al., 1995). The secretion of ATs, including intimin, by means of the Type-V secretion system (T5SS) involves the action of periplasmic chaperones and the β -barrel assembly machinery (BAM) complex, which catalyses their translocation across the OM (Albenne & Ieva, 2017; Wang et al., 2021). The periplasmic transit of intimin is mainly assisted by SurA chaperone, which maintains the polypeptide in an unfolded state until it is inserted into the OM in a process dependent on BamA (Bodelón et al., 2009). The process of intimin secretion is believed to take place through a hairpin-like intermediate where the N-terminus of the passenger is exported first by sequential folding of the passenger domain (Leo et al., 2016; Oberhettinger et al., 2015). The crystallographic data support this model, showing that the passenger and the β -barrel domain are connected by a linker located within the pore of the β -barrel (Fairman et al., 2012). Although the precise mechanism remains to be elucidated, biochemical and structural studies have provided evidence that translocation across the OM involves an assembly intermediate that consists in a hybrid barrel structure between the β -barrel of the AT and BamA, which functions as a polypeptide export channel (Doyle

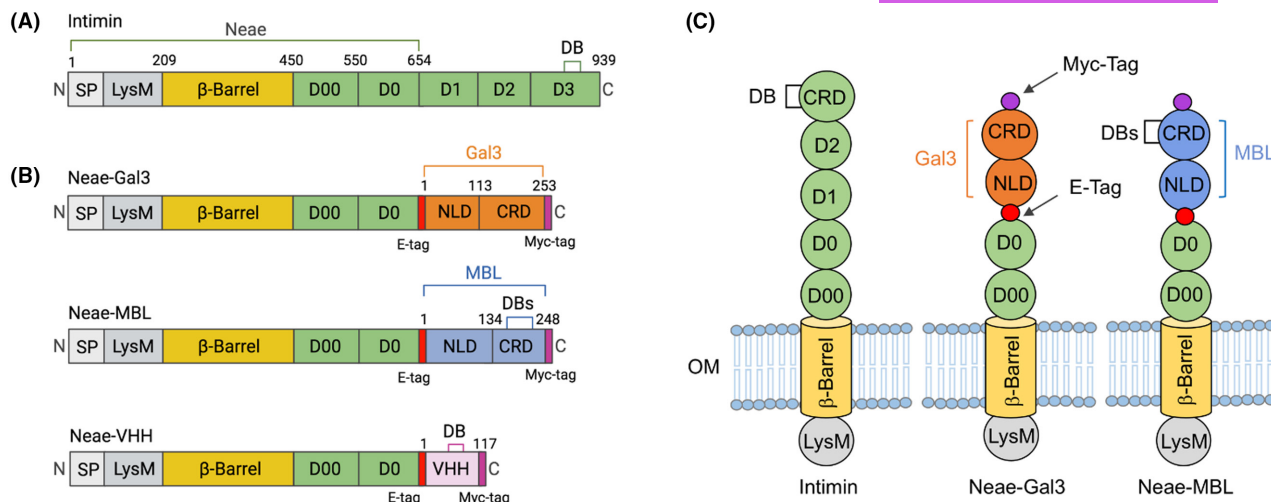


FIGURE 1 Domain organisation of the intimin bacterial display system for the expression of human lectins. (A) Scheme of intimin showing N-terminal signal peptide (SP), LysM, β -barrel for OM insertion, extracellular D00–D2 Ig-like domains and C-terminal lectin-like domain (D3). (B) Scheme of Neae-lectin fusions to Gal3 (Neae-Gal3), MBL (Neae-MBL) indicating the N-terminal non-lectin (NLD) and carbohydrate recognition (CRD) domains. The Neae-VHH fusion used as a control is also depicted. (C) Scheme of the structural domains of intimin, Neae-Gal3 and Neae-MBL in the bacterial OM. Amino-terminal (N) and carboxy (C)-terminal ends, intramolecular disulfide bond (DB), E-tag and Myc-tag epitopes are also indicated.

et al., 2022; Doyle & Bernstein, 2019, 2021; Tomasek et al., 2020). The Neae polypeptide (1–654 residues) of intimin, lacking D1, D2 and D3 domains, has proven to be an effective system for the bacterial display of a wide variety of heterologous passengers, including disulfide bond-containing peptides such as immunoglobulin domains and single-domain recombinant antibodies termed nanobodies (VHH) (Figure 1B; Adams et al., 2005; Alramahi et al., 2021; Piñero-Lambea et al., 2015; Salema et al., 2013, 2016; Wentzel et al., 2001). In this context, it has been estimated that the intimin bacterial display system allows the surface expression of approximately 8×10^3 nanobody molecules on each *E. coli* cell (Salema et al., 2013).

We focus this work on human galectin-3 (Gal3) and mannose-binding lectin (MBL) members of the galectin and Ca^{2+} -dependent (C-type) lectin families, respectively, which are the most populated classes of animal lectins (Bonnardel et al., 2019). Gal3 is a protein of approximately 30kDa that contains an amino-terminal non-lectin domain (NLD), and a carboxy-terminal CRD responsible for binding to galactosyl moieties, primarily *N*-acetylglucosamine (LacNAc) residues on glycoproteins (Sciacchitano et al., 2018). MBL is a protein of about 32kDa constituted by an NLD bearing a cysteine-rich, collagen and α -helical coiled-coil neck regions and a CRD that binds to mannose and *N*-acetylglucosamine sugar motifs (Sheriff et al., 1994). Structurally, MBL is an oligomer composed of three interlinked polypeptide chains stabilised by hydrophobic interactions and inter-chain disulfide bonds, which can be found in the human plasma as higher order oligomers (Jensen et al., 2005; Vang Petersen, 2001). The four cysteines in the CRD form two highly conserved intramolecular disulfide

bridges that are believed to play a role in the polypeptide folding (Weis et al., 1992; Zelensky & Gready, 2005). Unlike Gal3, which features a single cysteine residue, MBL was selected in this study to evaluate the suitability of the display system for the expression of human lectins containing disulfides. Structural information of both human lectins is shown in Section S3 (Figure S1A–D) and the domain architecture of the Gal3 and MBL fusions to Neae in Figure 1B,C.

Herein, we demonstrate that the Neae polypeptide allows the successful display of functional Gal3 and MBL on the surface of *E. coli*. The binding of the surface-expressed lectins was assessed by adhesion assays to cognate glycans and glycoconjugates immobilised on plastic surfaces and polymeric nanoparticles. We combined molecular dynamics (MD) simulation and bacterial display to explore the impact of point mutations in the glycan-binding activity of Gal3. We also investigated by mutagenesis the influence of the NLD and cysteine residues present in the CRD of MBL. Our findings give new insights into the functional properties of the mutants investigated and demonstrate the suitability and robustness of bacterial display for the expression and engineering of human lectins.

EXPERIMENTAL PROCEDURES

Bacterial strains and growth conditions

Escherichia coli strains used in the work are indicated in Section S1 (Table S1). *E. coli* cells were grown in Lysogeny broth (LB) (5g/L yeast extract, 10g/L tryptone and 10g/L NaCl) or in LB agar plates (1.5% w/v).

Induction of protein expression was performed in EcM1 bacteria grown for 18 h at 30°C without agitation in LB medium supplemented with D-glucose (2% w/v), chloramphenicol (30 µg/mL) and 0.05 mM isopropyl-β-D-thiogalactopyranoside (IPTG).

Plasmids, primers and cloning procedures

The plasmids and oligonucleotides (MilliporeSigma, Merck, Darmstadt, Germany) used in the present study are listed in [Tables S1](#) and [S2](#), respectively. Details of plasmid construction are described in [Section S2](#). Cloning procedures were performed following standard protocols of DNA digestion with restriction enzymes and ligation. PCRs for cloning purposes were performed with Vent DNA polymerase (NEB). All DNA constructs were sequenced by the Sanger method at CACTI-UVigo.

Protein extract preparation, SDS-PAGE and Western blot

Whole-cell protein extracts were prepared by mixing 100 µL of a bacterial suspension (OD_{600} of 1.5) in phosphate-buffered saline (PBS) with the same volume of sodium dodecyl sulfate (SDS) sample buffer (2×) or urea-SDS sample buffer (2×) as described previously ([Bodelón et al., 2009](#)). The samples were boiled for 10 min and loaded onto 10% SDS-PAGE gels, and electrophoresis was performed using the Mini-PROTEAN III system (Bio-Rad). For Western blot, the proteins were separated by SDS-PAGE and transferred to a 0.45 µm polyvinylidene difluoride (PVDF) membrane (Bio-Rad) using a Trans-Blot Turbo transfer system (Bio-Rad). For immunodetection, the PVDF membranes were probed with anti-Myc mAb clone 9B11 (1:2000; Cell Signaling Technology), anti-Gal3 mAb (1:1000; Abcam ab2785) or anti-MBL pAb (1:1000; ProSci 57-234) as indicated. Goat anti-mouse IgG-peroxidase (HRP) conjugate (1:2000; Abcam ab6789) and goat anti-rabbit IgG-peroxidase (HRP) conjugate (1:10,000; Sigma-Aldrich A0545) were used as secondary antibodies. Membranes were developed by chemiluminescence using a mixture of 100 mM Tris-HCl (pH 8.0) containing 1.25 mM luminol (Sigma-Aldrich), 0.22 mM coumaric acid (Sigma-Aldrich) and 0.0075% H_2O_2 (Sigma-Aldrich) and scanned in ChemiDoc XRS (Bio-Rad) and analysed using the Quantity One software (Bio-Rad).

Flow cytometry analysis

Escherichia coli bacteria corresponding to an OD_{600} of 0.5 were harvested from overnight LB cultures by

centrifugation (4000 g, 3 min), washed with PBS and re-suspended in 1 mL of PBS containing 3% (w/v) bovine serum albumin. After 30 min incubation at room temperature, anti-Galectin 3 or rabbit anti-E-tag (Abcam ab3397) antibodies were added (1:200) and incubated on ice for 1 h. Next, bacteria were washed in PBS, re-suspended in 0.5 mL of PBS containing 3% (w/v) bovine serum albumin and stained in the dark with either goat anti-rabbit Alexa 488 (1:500; Abcam ab150077) or anti-mouse Alexa 488 (1:500; Thermo Fisher Scientific A28175) for 40 min. Bacteria were washed three times with PBS and resuspended in 0.5 mL of PBS for analysis in a flow cytometer (CytoFLEX S, Beckman Coulter and Accuri C6; Becton Dickinson).

Adhesion assays to immobilised target glycans on plastic surfaces

Heparin sodium salt (1 mg/mL; Sigma-Aldrich H3393), Asialofetuin from foetal calf serum (1 mg/mL; Sigma-Aldrich A4781), D-(+)-Mannose (0.5 mg/mL; Sigma-Aldrich M8574), LacNAc (1 mg/mL; Sigma-Aldrich A7791) and SARS-CoV-2 Spike protein S1 (0.1 mg/mL; Thermo Fisher Scientific RP-87679) were adsorbed onto ELISA plates (MultiSorp, Thermo Fisher) at the indicated concentrations overnight at 4°C. For Gal3, coated plates were washed with PBS and blocked for 30 min at room temperature with PBS containing 3% (w/v) bovine serum albumin. Next, a bacterial suspension (100 µL) of the indicated strain was added at an OD_{600} of 3.0 in PBS and incubated for 1 h as previously described ([Piñero-Lambea et al., 2015](#)). For MBL, PBS was substituted by TBS buffer (50 mM Tris, 150 mM NaCl, pH 7.4) containing 5 mM $CaCl_2$. Bound bacteria were stained with 125 µL of 0.1% crystal violet (CV) solution (Sigma-Aldrich) for 15 min. Next, the plate was rinsed very gently with distilled water and CV was solubilised by applying 125 µL of 30% acetic acid in water to each well. The absorbance of CV was measured in a plate reader at 550 nm using 30% acetic acid as blank. The binding assays in multiwell format were performed at least three times each.

Synthesis of Man-PEI polymeric nanoparticles

The procedure was performed as described elsewhere ([Li et al., 2019](#)). Briefly, 2 mL of branched polyethylenimine MW 10,000 (Polysciences) (0.1 g/mL) was added to 14 mL of TBS 5 mM $CaCl_2$ and stirred for 1 min. Then, 4 mL of D-(+) mannose (0.1 M) (Sigma-Aldrich) was added and stirred for 1 additional min. The mixture was heated at 90°C for 40 min, and the Man-PEI nanoparticles were purified by dialysis with a 10 kDa cutoff bag in ultrapure water for 36 h.

Fluorescent detection of bacterial cells bound to Man-PEI nanoparticles

The Man-PEI NP solution (1 mL) was added to a bacterial suspension in TBS 5mM CaCl₂ bearing the indicated OD_{600nm} and incubated for 1 h at 37°C with gentle agitation (160 rpm). Next, bacteria were washed twice with distilled water by centrifugation at 4000 g for 3 min, and the fluorescence spectra were recorded with an excitation wavelength of 340 nm (Li et al., 2019).

Molecular dynamics simulations

The binding of Gal3 and three mutated versions of the protein to LacNAc was studied by means of molecular dynamics (MD) simulations. Taking as starting point the crystal structure of Gal3 bound to LacNAc (PDB ID: 1KJL) without crystal-water molecules, we prepared the mutants R186A (Gal3_{M1}), R186A, E165A (Gal3_{M2}) and R186A, E165A, R162A, E184A (Gal3_{M3}) and placed each complex in the centre of a cubic box extending 10 Å from the protein and solvated with around 9000–9500 water molecules. The protonation states of all residues are those employed in previous studies (Saraboji et al., 2011), and potassium and chloride ions were added to maintain electroneutrality. Molecular dynamics were performed using GROMACS 2021.3 (Abraham et al., 2015). Both the protein and the LacNAc ligand were described using the CHARMM36 force field, and TIP3P was chosen as model for water molecules (Guvench et al., 2011). For each complex, initial energy minimisation was performed until the maximum force was smaller than 10 kJ/mol/nm followed by 100 ps of NVT and NPT equilibrations, respectively. The V-rescale thermostat with a relaxation time of 1.0 ps and the Parrinello-Rahman barostat with a coupling constant of 2 ps were used to maintain the average temperature of the system at 300 K and a constant pressure of 1 bar. At least five independent production runs of 10 ns length were performed for each system. To characterise the binding interaction between Gal3 and its mutants with the LacNAc ligand, we computed the binding free energy employing the Molecular Mechanics Generalized Born Surface Area (MM/GBSA) method (Kollman et al., 2000; Srinivasan et al., 1998) using the gmx_MMPBSA tool (Valdés-Tresanco et al., 2021).

RESULTS AND DISCUSSION

Surface display and functional activity of Gal3

As a host for cell surface display, we employed an *E. coli* K-12 strain termed EcM1 (Table S1). This strain has a deletion in the operon encoding type 1 fimbriae (Δ *fim*) (Munera et al., 2008), an adhesin involved in the

recognition and binding to mannose moieties on glycoproteins (Lupo et al., 2021). The rationale for using bacterial cells devoid of type 1 fimbriae is to avoid potential interferences with the surface-displayed lectins in the binding assays.

Initially, we assessed the expression of Neae-Gal3 by SDS-PAGE and Western blot after induction with IPTG (see Experimental Procedures). As a control, we included a Neae fusion to a nanobody (Neae-VHH), which has been reported to be efficiently displayed on the bacterial surface (Salema et al., 2013). As shown in Figure 2A, it is observed a band of approximately 70 kDa in whole-cell protein extracts from the induced cells that corresponds to Neae-Gal3 (Figure 2A, compare lanes 3 and 4). The surface display of Gal3 was also evaluated by immunodetection of the Myc-tag in intact cells followed by flow cytometry. To this aim, un-induced and induced bacteria bearing pNeae-Gal3, or pNeae-VHH plasmids, were stained with anti-Myc mAbs followed by anti-mouse IgG-Alexa488. In the flow cytometry histograms shown in Figure 2B, it is observed that induced cells expressing either Neae-Gal3 or Neae-VHH show a mean fluorescence intensity up to 100-fold higher than that of non-induced cells. Notably, the presence of a single peak in the flow cytometry histogram indicates that most cells expressed homogenous levels of the fusion proteins.

The binding activity of the surface-displayed Gal3 was assessed by means of a crystal violet assay in microtitre plates coated with LacNAc, heparin or asialofetuin (ASF). These ligands are known to bind the carbohydrate-binding site of the lectin (Lepur et al., 2012; Seetharaman et al., 1998; Talaga et al., 2016). IPTG-induced EcM1 bacteria bearing pNeae-Gal3 or pNeae-VHH plasmids were incubated on ligand-coated microtitre plates. Next, bound bacteria were stained with crystal violet, and the absorbance of the solubilised dye was evaluated spectrophotometrically (see Experimental Procedures). As shown in Figure 2C, the expression of Neae-Gal3 induced the binding of bacterial cells to the different galectin ligands at similar levels, whereas the expression of Neae-VHH produced negligible levels of adhesion, demonstrating the activity of the surface-expressed Gal3, as well as the selectivity of the system.

Structural and functional analysis of Gal3 mutants

Having demonstrated the functional activity of the displayed Gal3, we next sought to evaluate point mutations in the CRD of the lectin and how they affect the binding to cognate ligands. This domain folds into two antiparallel β -sheets of six (S1–S6) and five (F1–F5) strands forming a β -sheet sandwich structure bearing the canonical carbohydrate-binding pocket

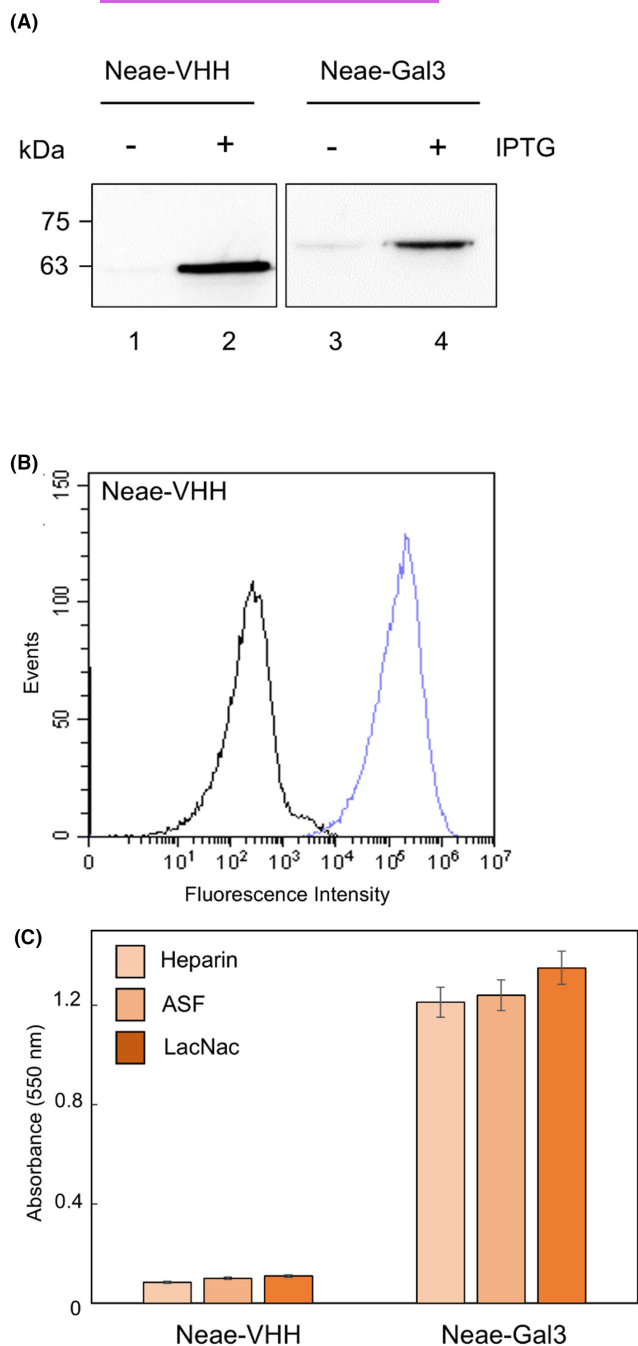


FIGURE 2 Analysis of bacterial surface display and functional activity of Neae-Gal3. (A) Western blot of bacteria expressing Neae-VHH or Neae-Gal3 induced (+) or not (-) with IPTG and probed with anti-Gal3 antibodies. (B) Flow cytometry analysis of uninduced (black line) and IPTG-induced (blue and orange lines) bacteria transformed with pNeae-VHH or pNeae-Gal3, respectively. Histograms show the fluorescence intensity of bacteria stained with anti-Myc tag (for Neae-VHH) or anti-Gal3 antibodies and secondary anti-mouse IgG-Alexa 488. (C) Absorbance at 550 nm of crystal violet-stained bacteria expressing Neae-VHH or Neae-Gal3 bound to microtitre wells coated with different Gal3 ligands: LacNac, heparin and ASF. Error bars indicate standard deviations.

(Seetharaman et al., 1998). Structural studies of Gal3 bound to the prototypical ligand LacNac show that

the galactose (GAL) unit of the disaccharide is most deeply buried in the binding site forming hydrogen bonds with Arg-144, His-158, Asn-160, Arg-162, Asn-174 and Glu-184, as well as a stacking interaction with Trp-181. The *N*-acetylglucosamine (NAG) moiety of LacNac is more solvent-exposed and hydrogen bonds to Arg-162, Glu-165 and Glu-184 (Figure 3A, Gal3) (Chan et al., 2018; Seetharaman et al., 1998). We focused the mutation analysis on the amino acid residues Arg-162, Glu-165, Glu-184 and Arg-186, which are involved in a highly conserved salt bridge network that has been proposed to play a significant role in carbohydrate recognition of Gal-1, -3 and -7 lectins towards LacNac (St-Pierre et al., 2015). Initially, we applied molecular dynamics (MD) to investigate the effect of loss-of-function mutations in the above-indicated amino acid residues in their interaction with LacNac. We carried out MD simulations of the complexation of the disaccharide into the CRD of wild-type Gal-3 and three mutated versions: Gal3_{M1} (R186A), Gal3_{M2} (R186A, E165A) and Gal3_{M3} (R186A, E184A, E165A, R162A) (Figure 3 and Figure S3A–F). In general, by gradually increasing the number of mutations we observe that LacNac loses direct hydrogen bonding with the carbohydrate binding pocket and rotates its conformation (Figure 3A,B and more detailed information in Tables S3–S5 and Figures S2–S6). The binding interaction between Gal3 and its mutants with the LacNac ligand was also analysed by computing the binding free energy (ΔG_{bind}) through the Molecular Mechanics Generalized Born Surface Area (MM/GBSA) method (Srinivasan et al., 1998). The results show a gradual decrease of ΔG_{bind} , reflecting that the interaction with the CRD is weakened as the number of mutations increases (Figure 3C, Table S4 and Figure S5). Interestingly, it can be observed that the interaction between the binding pocket and the GAL unit of the ligand is maintained, while the NAG moiety diverges notably from the initial disposition of LacNac in the wild type. Also, we noticed that the R186A mutation in Gal3_{M1} results in the loss of the water-mediated hydrogen bond with LacNac mediated by Glu-165. The double mutation in Gal3_{M2} (R186A, E165A) did not elicit a significant alteration of the interaction with the disaccharide as compared by visual inspection with Gal3_{M1} (R186A) (Figure 3A,B). Nevertheless, ΔG_{bind} quantification demonstrates the weaker binding of Gal3_{M2} vs Gal3_{M1} (Figure 3C). Additionally, simulations with longer production times even indicated that the interaction between LacNac and the mutated systems might be lost and, as a consequence, the ligand does not remain attached to the CRD region (Table S5 and Figure S6). However, it must be taken into account here that MD simulations only consider a single ligand-protein interaction and the possibility of oligomerisation or multivalent behaviour of Gal3 might be recalled to explain

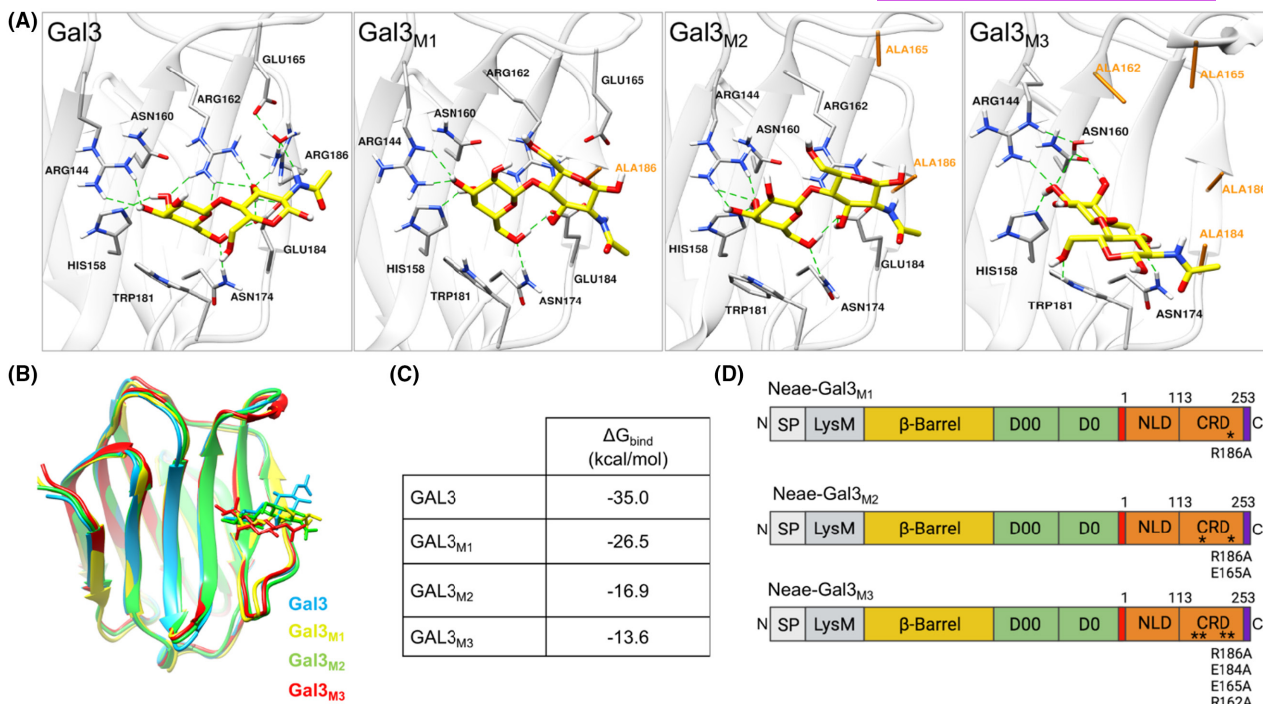


FIGURE 3 Molecular dynamics simulation analysis of point mutants of Gal3 glycan-binding pocket. (A) Selected MD snapshots for the interacting residues of Gal3 with LacNAc in its native bound pose, as well as the indicated mutants. (B) Superimposed images of LacNAc interacting with Gal3 and its mutants. (C) Binding free energy, ΔG_{bind} , between LacNAc and Gal3 and its three mutants. (D) Scheme of the Gal3 mutants fused to Neae bacterial display system. The asterisks shown in the lectin CRD indicate the relative position of the mutated amino acid residues.

experimental affinities. Additional data, discussion and bibliographic references regarding MD results are shown in Sections S4 and S6, respectively.

Next, we generated the different Neae-Gal3_{M1}, Gal3_{M2} and Gal3_{M3} fusions (Figure 3D) aiming to evaluate their binding to cognate ligands by bacterial display. In the Western blot analysis of whole-cell protein extracts from IPTG-induced cultures, it can be observed protein bands with the expected size for the three mutants (Figure 4A). The flow cytometry analysis shows that all of them were detected at similar levels as the wild-type Neae-Gal3 (compare Figures 4B and 2D). Once we demonstrated that the Gal3 mutants were efficiently expressed on the cell surface, we assessed their capacity to bind LacNAc, heparin and ASF immobilised on microtitre plates by crystal violet staining. This assay shows that, as compared to Neae-Gal3, the expression of Neae-Gal3_{M1}, Neae-Gal3_{M2} and Neae-Gal3_{M3} reduced bacterial adhesion to the ligands in ca. 10%, 25% and 40%, respectively (Figure 4C). This trend is in good agreement with the results obtained by MD (Figure 3C and Table S4). The reduction of binding activity to LacNAc and ASF observed for the single mutation R186A in Neae-Gal3_{M1} is in accordance with the findings reported by others employing purified Gal3 bearing a R186S point mutation (Lepur et al., 2012; Salomonsson et al., 2010). Remarkably, the expression of the Neae-Gal3_{M3} fusion did not completely abolish the interaction

between Gal3 and the disaccharide (Figure 4C). As expected, mutation of the 4 amino acid residues in Neae-Gal3_{M3} mainly affects the interaction with the NAG ring, while the GAL moiety can still form hydrogen bonds with Arg-144, His-158, Asn-160 and Asn-174, as well as the stacking interaction with Trp-181 (Figure 3). Therefore, we can conclude that the amino acid residues involved in the salt-bridge network are not major determinants of the binding between the lectin and the disaccharide.

Surface display and functional activity of MBL

To broaden the application of this approach to disulfide bond-containing lectins, we investigated the bacterial display of human MBL. The NLD contains a cysteine-rich region that participates in interchain disulfide bonds that hold MBL oligomers together (Larsen et al., 2004; Sheriff et al., 1994; Vang Petersen, 2001). The CRD features four highly conserved cysteines that form two intramolecular disulfide bridges (Cys-155/Cys-244 and Cys-222/Cys-236), which are believed to contribute to the stabilisation of the overall fold of the sugar-binding domain (Weis et al., 1992; Zelensky & Gready, 2005). To our knowledge, assessment of the influence of the above-mentioned cysteines in the glycan-binding

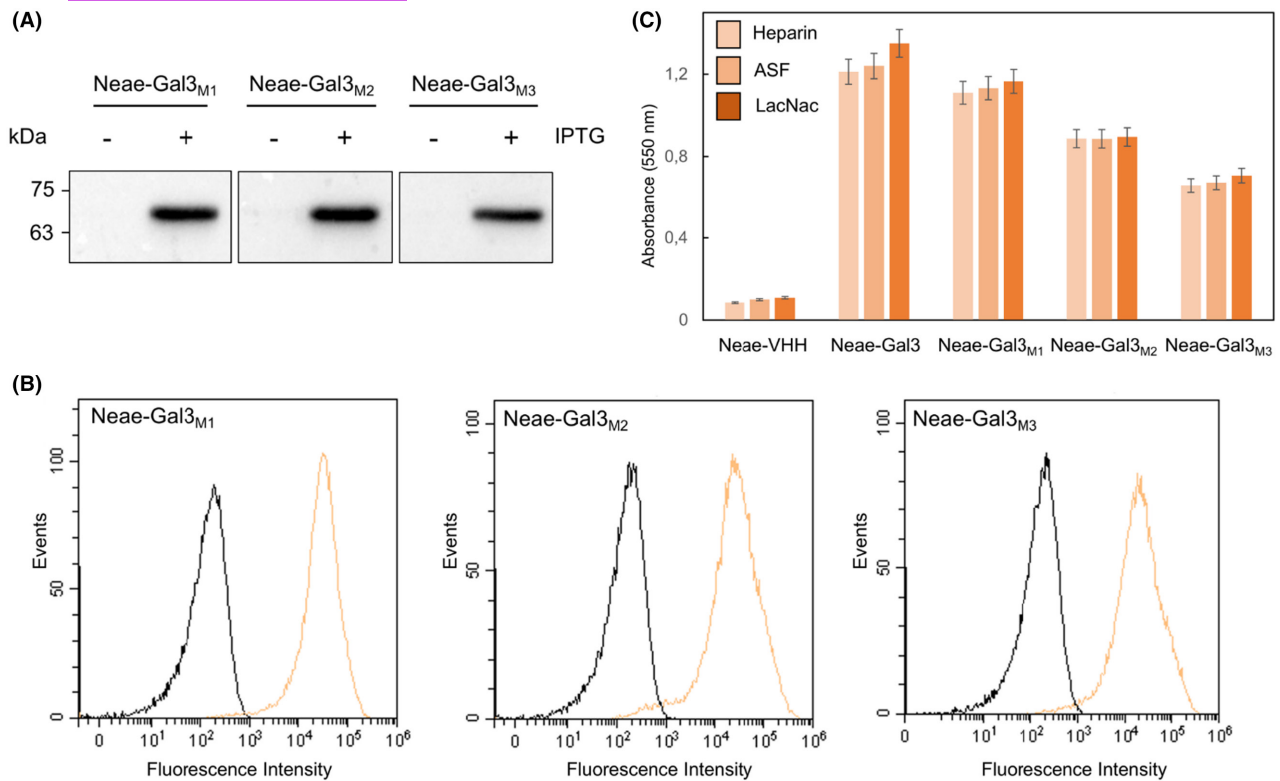


FIGURE 4 Analysis of bacterial surface display and functional activity of Gal3 mutants. (A) Western blot of bacteria expressing the different Neae-Gal3 mutants induced (+) or not (-) with IPTG and probed with anti-Gal3 mAbs. (B) Flow cytometry analysis of uninduced (black line) and IPTG-induced (orange line) bacteria transformed with control pNeae-Gal3 or its different mutants. Histograms show the fluorescence intensity of bacteria stained with anti-Gal3 mAbs and secondary anti-mouse IgG-Alexa 488. (C) Absorbance at 550 nm of crystal violet-stained bacteria expressing Neae-VHH, Neae-Gal3 and the different mutants bound to microtitre wells coated with the different Gal3 ligands: LacNac, heparin and ASF. Error bars indicate standard deviations. The binding assays in multiwell format were performed at least three times each.

activity of human MBL has not been addressed to date. To this end, we assessed the display and functional activity of a MBL deletion mutant devoid of the NLD termed Neae-MBL_{CRD}, which therefore is unable to form interchain oligomers. In addition, we generated a Neae-MBL_{ΔCys} fusion in which two cysteines of the CRD were replaced by alanine residues (C222A, C244A) to abrogate the formation of the two canonical intramolecular disulfide bonds (Figure 5A). The expression of Neae-MBL, Neae-MBL_{CRD} and Neae-MBL_{ΔCys} was analysed by Western blot with antibodies against MBL in total cell extracts. As shown in Figure 5B, Neae-MBL_{CRD} is expressed at higher levels than Neae-MBL and Neae-MBL_{ΔCys} polypeptides. We next assessed the surface expression of the different Neae-MBL fusions by flow cytometry employing mAbs against the E-tag localised at the N-terminal region of the passenger (Figure 1), as the mAbs used to immunodetect the Myc-tag in Neae-VHH (Figure 2B) did not recognise the C-terminal epitope in the three different Neae-MBL fusions evaluated (not shown). This result suggested that the Myc-tag epitope might be hidden in the surface-displayed polypeptides and, therefore, it cannot be bound by the mAbs. Alternatively, neighbouring

sequences to the Myc-tag might affect its recognition by the antibody as the 9B11 clone employed in this assay shows context-dependent differences in its ability to bind N- or C-terminal Myc-tagged proteins (Schüchner et al., 2020). For immunodetection of the E-tag, IPTG-induced *E. coli* cells harbouring pNeae-MBL, pNeae-MBL_{CRD} or pNeae-MBL_{ΔCys} were incubated with anti-E-tag mAbs followed by anti-mouse IgG-Alexa488. The flow cytometry analysis shows that all three polypeptides were successfully recognised by the E-tag mAbs (Figure 5C) suggesting that the Neae-MBL fusions are present in the cell surface. In addition, this result shows that Neae-MBL and Neae-MBL_{CRD} are expressed at higher levels than Neae-MBL_{ΔCys}, which is in accordance with the Western blot results (Figure 5B).

The functional activity of the surface-displayed MBL, as well as their mutated versions, was investigated by adhesion assays on microtitre plates coated with either mannose or the spike protein of severe acute respiratory syndrome-coronavirus 2 (SARS-CoV-2), which has been reported to be bound by this lectin (Stravalaci et al., 2022). The expression of Neae-MBL elicited the adhesion of bacteria to both mannose and spike protein (Figure 5D), whereas

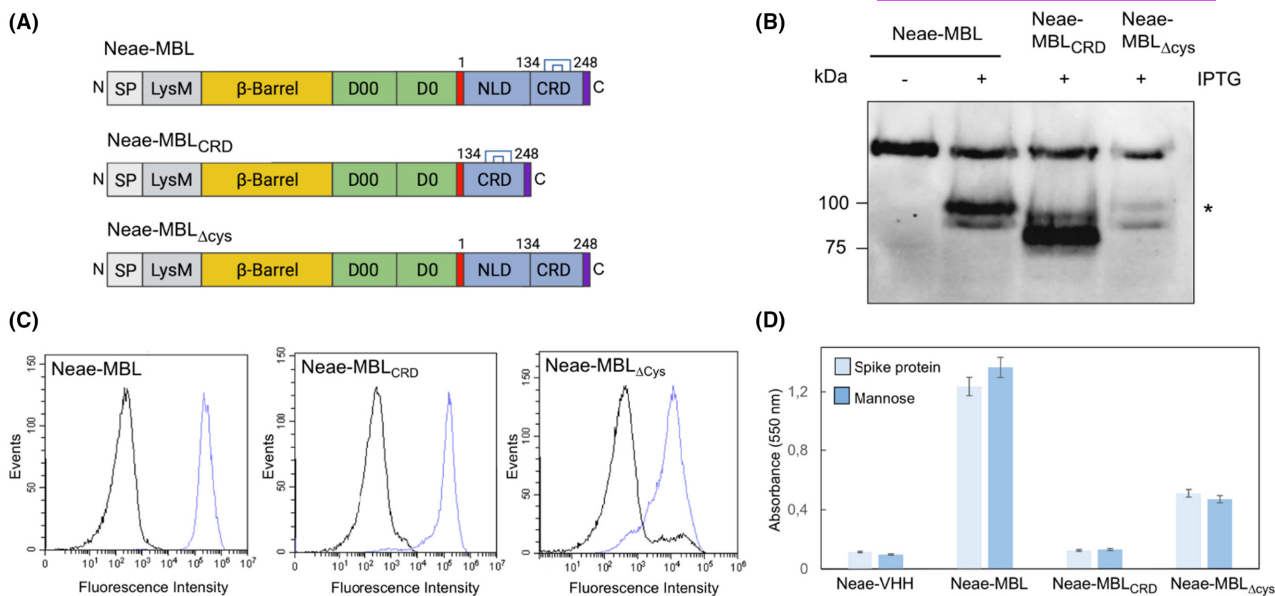
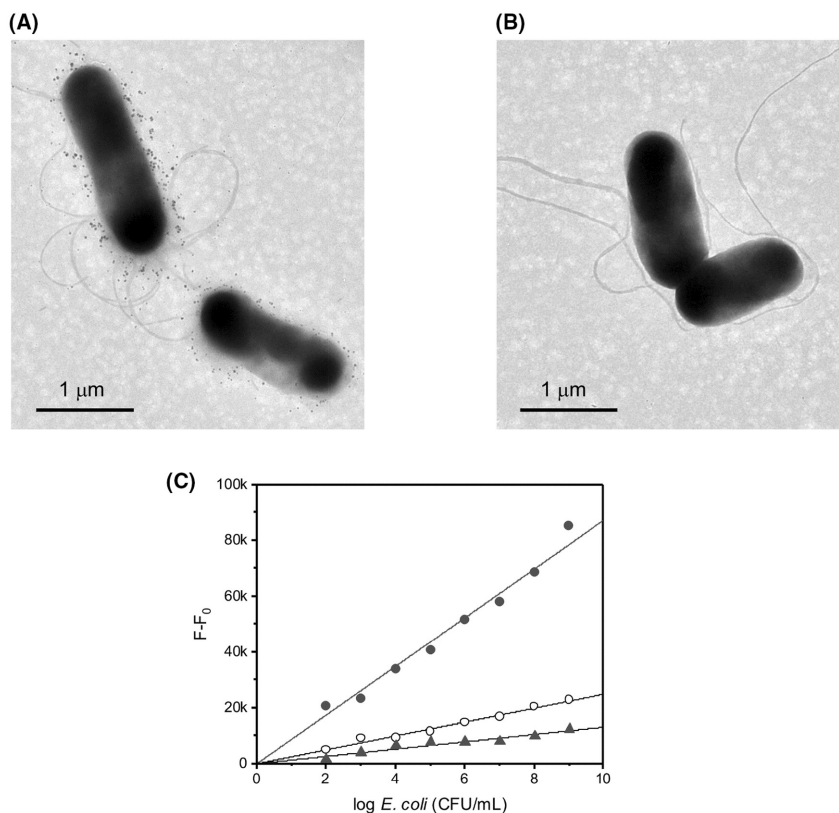


FIGURE 5 Analysis of bacterial surface display and functional activity of MBL. (A) Scheme of Neae-MBL, Neae-MBL_{CRD} and Neae-MBL_{ΔCys}. (B) Western blot of bacteria expressing the indicated Neae-MBLs fusions induced (+) or not (-) with IPTG and probed with rabbit anti-MBL and goat anti-rabbit HRP. Asterisk indicates the protein bands corresponding to the different Neae-MBL fusions. (C) Flow cytometry analysis of uninduced (black line) and IPTG-induced (blue line) bacteria transformed with pNeae-MBL, pNeae-MBL_{CRD} or pNeae-MBL_{ΔCys}. Histograms show the fluorescence intensity of bacteria stained with anti-E-tag antibody and secondary anti-mouse IgG-Alexa 488. (D) Absorbance at 550 nm of crystal violet-stained bacteria expressing Neae-MBL, Neae-MBL_{CRD} or Neae-MBL_{ΔCys}, bound to microtitre wells coated with SARS-CoV-2 spike protein or mannose. Error bars indicate standard deviations. The binding assays in multiwell format were performed at least three times each.

FIGURE 6 MBL-mediated bacterial adhesion to Man-PEI nanoparticles. (A, B) TEM images of EcM1 bacteria expressing Neae-MBL (A) and Neae-VHH (B). (C) Net increase of fluorescence, $F - F_0$, as a function of bacterial concentration (CFU/mL) of Neae-MBL (black circles), Neae-MBL_{CRD} (black triangles) and Neae-MBL_{ΔCys} (empty circles). The lines represent the best fit of a linear equation to the experimental data.



the display of Neae-MBL_{ΔCys} significantly reduced the adhesion to both ligands by approximately 60%. This result could be attributed to the low expression

levels of this polypeptide and suggests that the mutated cysteines may be involved in the binding activity of the lectin. Expression of Neae-MBL_{CRD} did not

promote bacterial adhesion to any of the two ligands, demonstrating that the NLD region is absolutely required for carbohydrate binding in the display system (Figure 5D).

We sought to test the functional activity of the surface-displayed MBLs by an additional method that involves the use of 30 nm polyethyleneimine copolymer nanoparticles functionalised with mannose (Man-PEI) (Section S5, Figure S7A–D; Li et al., 2019). Since the Man-PEI nanoparticles emit a bright blue fluorescence when illuminated with UV light, we harnessed this property of the nanomaterial to assess the binding of the lectin to the mannose moiety by fluorescence spectroscopy. IPTG-induced EcM1 bacteria bearing pNeae-MBL, or control pNeae-VHH, were incubated with the Man-PEI nanoparticles, and after removing unbound nanoparticles by centrifugation, the samples were analysed by transmission electron microscopy (TEM) (Figure 6A,B and Figures S8 and S9). The microscopy images show the presence of nanoparticles bound to the bacterial cells that express Neae-MBL (Figure 6A and Figure S8) and not to control bacteria (Figure 6B and Figure S9), demonstrating the binding specificity of the surface-displayed lectin. Consequently, we applied this strategy to evaluate the mannose-binding activity of the different MBL fusions in bacterial cells expressing Neae-MBL, Neae-MBL_{ΔCys} or Neae-MBL_{CRD}. To this aim, a fixed amount of the Man-PEI nanoparticles was incubated with increasing bacterial concentrations, and the presence of Man-PEI/EcM1 conjugates was determined by fluorescence spectroscopy (see Experimental Procedures). As shown in Figure 6C, the highest fluorescence intensities were obtained by the bacterial display of Neae-MBL (black circles), whereas expression of Neae-MBL_{ΔCys} (empty circles) yielded intensities slightly higher than those of Neae-MBL_{CRD} (black triangles). These results are in good agreement with the plate adhesion assay (Figure 5D). The linear relationship observed between the fluorescence intensity and the concentration of *E. coli* bacteria expressing the different fusion proteins is indicative of the reliability of the assay.

Our results demonstrate that the intimin display system can express functional MBL on the bacterial surface. In its native form, human MBL is a homotrimer that can further oligomerise to form biologically active high-order structures. Oligomerisation of MBL is mediated by cysteine residues present in the NLD-rich domain that form intra- and intersubunit disulfide bonds (Larsen et al., 2004; Sheriff et al., 1994). The deletion of the NLD region in Neae-MBL_{CRD} does not affect its expression and surface display; nevertheless, it completely abolished glycan binding. These findings suggest that deletion of this amino-terminal region reduces the capacity of the CRD to interact with its glycan targets, possibly due to steric hindrance, and/or might prevent it from adopting a proper

orientation for efficient ligand binding (Takahashi & Ezekowitz, 2005). Also, this result raises the intriguing possibility that the surface-displayed MBL might require an oligomeric conformation for activity triggered by the NLD. There are three possible scenarios in which oligomerisation of Neae-MBL could take place (i) in the periplasmic space; (ii) during OM translocation; and (iii) after translocation of individual subunits. In general, the secretion of ATs imposes structural constraints and the polypeptide must adopt a folding competent state for translocation (Meuskens et al., 2019). Experimental evidence has shown that both the size and structural complexity are key factors that limit the export of heterologous passenger domains (van Ulsen et al., 2014). Despite some local tertiary folding is tolerated for some ATs, including the disulfide bond present in the C-type lectin domain of intimin (see below), engineered disulfides between spatially distant cysteines can block secretion (Jong et al., 2007; Leyton et al., 2011). Therefore, since translocation of AT can be affected by the folding state of the passenger domain in the periplasm, it is very unlikely that preformed oligomers of Neae-MBL can be translocated across the OM. Interestingly, purified intimin can form dimers, a property that has been attributed to its β -barrel and periplasmic LysM domains (Leo et al., 2015; Touzé et al., 2004). The formation of Neae-MBL oligomers during translocation seems very doubtful as it would imply that a single BamA protein would have to catalyse the simultaneous insertion of multiple β -barrels. In this regard, analysis by super-resolution imaging experiments revealed the existence of multiple BAM complexes that colocalise in discrete membrane precincts, which participate in the assembly of OmpC trimers (Gunasinghe et al., 2018). Interestingly, the reconstitution of OmpC assembly in vitro showed that the BAM complex catalyses the integration of individual subunits in the membrane in a stepwise fashion (Hussain et al., 2021). Thus, in a more plausible scenario, we can speculate that Neae-MBL would be secreted to the cell surface as monomers and the passengers would then form oligomers with neighbouring surface-exposed Neae-MBLs.

The intimin display system allows to efficiently secrete a repertoire of disulfide-containing proteins such as EETI-CK, IL-4 and REIv (Wentzel et al., 2001), as well as nanobodies (Salema & Fernández, 2017) in *E. coli*. Herein, we demonstrated that this display platform allows the expression of functional human MBL in the bacterial surface. Structural data show that the CRD of the lectin folds in a double loop stabilised by two highly conserved intramolecular disulfide bonds (Cys-155/Cys-244 and Cys-222/Cys-236) (Weis et al., 1992), which is characteristic of the C-type lectin-like domain superfamily (Zelensky & Gready, 2005). The Cys-155/Cys-244 pair links the N- to the C-terminal end of the folded polypeptide, while the Cys-222/Cys-236 disulfide

stabilises a long loop which is believed to be involved in saccharide binding (Zelensky & Greedy, 2005). Mutation of two cysteine residues to alanines (C222A, C244A) that participate in the intramolecular disulfides of the CRD significantly reduced the expression levels of Neae-MBL_{ΔCys} (Figure 5B,C), as well as its binding capability towards immobilised glycans (Figures 5D and 6C). These findings point towards the involvement of the cysteine residues, and potentially the disulfide bonds, in the lectin's functional activity. Interestingly, the C-type lectin domain of intimin contains two cysteine residues forming an intra-domain disulfide bond. Expression of intimin in an *E. coli dsbA* mutant showed lower display levels on the cell surface and elicited the polypeptide less stable and susceptible to protease digestion, likely due to the misfolding of the secreted C-type lectin domain. An alkylation assay comparing wild-type and *dsbA* mutant provided direct evidence of the formation of this disulfide bond by DsbA (Bodelón et al., 2009) Whether the intramolecular Cys-155/Cys-244 and Cys-222/Cys-244 disulfide bridges are formed in the CRD of the surface-displayed MBL, or not, and whether they are catalysed by Dsb proteins await further investigation.

CONCLUSIONS

We established for the first time bacterial display for the expression of human lectins. As shown herein, functional Gal3 and MBL were successfully expressed in the bacterial surface, thereby providing a new display platform for the engineering of human lectins. In combination with MD simulations, the structure-based site-directed mutagenesis showed that increasing mutations in the amino acid residues Arg-162, Glu-165, Glu-184 and Arg-186 present in the carbohydrate-binding pocket of Gal3 gradually decrease its affinity towards target glycans. The cell surface display of MBL indicates the suitability of the proposed method for disulfide bond-containing lectins. We demonstrated that the NLD region of MBL is completely required for glycan binding, and mutation of Cys-222 and Cys-244 reduced the expression levels and binding activity, pointing towards a role of these amino acid residues in the folding stability of the lectin. This work showcases bacterial display as a novel approach for the surface expression and engineering of human lectins with great potential to generate useful glycan binders with enhanced affinity, selectivity and specificity.

AUTHOR CONTRIBUTIONS

Alba Vazquez-Arias: Conceptualization (equal); data curation (equal); formal analysis (equal); funding acquisition (equal); investigation (lead); methodology (lead); project administration (equal); resources (equal); software (equal); supervision (equal); validation (equal);

visualization (equal); writing – original draft (equal); writing – review and editing (equal). **Lorena Vázquez-Iglesias:** Conceptualization (equal); data curation (equal); formal analysis (equal); funding acquisition (equal); investigation (equal); methodology (supporting); project administration (equal); software (equal); supervision (equal); validation (equal); visualization (equal); writing – original draft (equal); writing – review and editing (equal). **Ignacio Perez-Juste:** Conceptualization (equal); data curation (equal); formal analysis (equal); funding acquisition (equal); investigation (equal); methodology (equal); project administration (equal); resources (equal); software (equal); supervision (equal); validation (equal); visualization (equal); writing – original draft (equal); writing – review and editing (equal). **Jorge Perez-Juste:** Conceptualization (equal); data curation (equal); formal analysis (equal); funding acquisition (equal); investigation (equal); methodology (equal); project administration (equal); resources (equal); software (equal); supervision (equal); validation (equal); visualization (equal); writing – original draft (equal); writing – review and editing (equal). **Isabel Pastoriza-Santos:** Conceptualization (equal); data curation (equal); formal analysis (equal); funding acquisition (equal); investigation (equal); methodology (equal); project administration (equal); resources (equal); software (equal); supervision (equal); validation (equal); visualization (equal); writing – original draft (equal); writing – review and editing (equal). **Gustavo Bodelon:** Conceptualization (lead); data curation (equal); formal analysis (equal); funding acquisition (equal); investigation (lead); methodology (equal); project administration (equal); resources (equal); software (equal); supervision (lead); validation (equal); visualization (equal); writing – original draft (lead); writing – review and editing (lead).

ACKNOWLEDGEMENTS

The authors acknowledge financial support from the European Innovation Council (Horizon 2020 Project: 965018 – BIOCELLPHE) and the Spanish Ministry of Science and Innovation (grants PID2019-109669 RB-I00, PID2019-108954RB-I00, and PID2022-138023NB-I00). G.B. acknowledges financial support from the Xunta de Galicia (Centro singular de investigación de Galicia accreditation 2019–2022) and the European Union (European Regional Development Fund – ERDF).

FUNDING INFORMATION

No funding information provided.

CONFLICT OF INTEREST STATEMENT

There are no conflicts of interest to declare.

ORCID

Gustavo Bodelon  <https://orcid.org/0000-0003-2815-7635>

REFERENCES

- Abraham, M.J., Murtola, T., Schulz, R., Páll, S., Smith, J.C., Hess, B. et al. (2015) GROMACS: high performance molecular simulations through multi-level parallelism from laptops to supercomputers. *SoftwareX*, 1–2, 19–25.
- Adams, T.M., Wentzel, A. & Kolmar, H. (2005) Intimin-mediated export of passenger proteins requires maintenance of a translocation-competent conformation. *Journal of Bacteriology*, 187, 522–533.
- Albenne, C. & Ieva, R. (2017) Job contenders: roles of the β -barrel assembly machinery and the translocation and assembly module in autotransporter secretion. *Molecular Microbiology*, 106, 505–517.
- Al-ramahi, Y., Nyerges, A., Margolles, Y., Cerdán, L., Ferenc, G., Pál, C. et al. (2021) ssDNA recombineering boosts in vivo evolution of nanobodies displayed on bacterial surfaces. *Communications Biology*, 4, 1169.
- André, S., Kaltner, H., Manning, J., Murphy, P. & Gabius, H.-J. (2015) Lectins: getting familiar with translators of the sugar code. *Molecules*, 20, 1788–1823.
- Batchelor, M. (2000) Structural basis for recognition of the translocated intimin receptor (Tir) by intimin from enteropathogenic *Escherichia coli*. *The EMBO Journal*, 19, 2452–2464.
- Bodelón, G., Marín, E. & Fernández, L.A. (2009) Role of periplasmic chaperones and BamA (YaeT/Omp85) in folding and secretion of intimin from enteropathogenic *Escherichia coli* strains. *Journal of Bacteriology*, 191, 5169–5179.
- Bonnardel, F., Mariethoz, J., Pérez, S., Imberty, A. & Lisacek, F. (2021) LectomeXplore, an update of UniLectin for the discovery of carbohydrate-binding proteins based on a new lectin classification. *Nucleic Acids Research*, 49, 1548–1554.
- Bonnardel, F., Mariethoz, J., Salentin, S., Robin, X., Schroeder, M., Perez, S. et al. (2019) UniLectin3D, a database of carbohydrate binding proteins with curated information on 3D structures and interacting ligands. *Nucleic Acids Research*, 47, 1236–1244.
- Broussard, A.C., Boyce, M. & Bement, W. (2019) Life is sweet: the cell biology of glycoconjugates. *Molecular and Cellular Biology*, 30, 525–529.
- Cecioni, S., Imberty, A. & Vidal, S. (2014) Glycomimetics versus multivalent glycoconjugates for the design of high affinity lectin ligands. *Chemical Reviews*, 115, 525–561.
- Çelik, E., Fisher, A.C., Guarino, C., Mansell, T.J. & DeLisa, M.P. (2010) A filamentous phage display system for N-linked glycoproteins. *Protein Science*, 19, 2006–2013.
- Chan, Y.-C., Lin, H.-Y., Tu, Z., Kuo, Y.-H., Hsu, S.-T. & Lin, C.-H. (2018) Dissecting the structure–activity relationship of galectin–ligand interactions. *International Journal of Molecular Sciences*, 19, 392.
- Chettri, D., Boro, M., Sarkar, L. & Verma, A.K. (2021) Lectins: biological significance to biotechnological application. *Carbohydrate Research*, 506, 108367.
- Coelho, L.C.B.B., Silva, P.M.S., Lima, V.L.M., Pontual, E.V., Paiva, P.M.G., Napoleão, T.H. et al. (2017) Lectins, interconnecting proteins with biotechnological/pharmacological and therapeutic applications. *Evidence-Based Complementary and Alternative Medicine*, 2017, 1–22.
- Dang, K., Zhang, W., Jiang, S., Lin, X. & Qian, A. (2020) Application of lectin microarrays for biomarker discovery. *ChemistryOpen*, 9, 285–300.
- Doyle, M.T. & Bernstein, H.D. (2019) Bacterial outer membrane proteins assemble via asymmetric interactions with the BamA β -barrel. *Nature Communications*, 10, 3358.
- Doyle, M.T. & Bernstein, H.D. (2021) BamA forms a translocation channel for polypeptide export across the bacterial outer membrane. *Molecular Cell*, 81, 2000–2012.
- Doyle, M.T., Jimah, J.R., Dowdy, T., Ohlemacher, S.I., Larion, M., Hinshaw, J.E. et al. (2022) Cryo-EM structures reveal multiple stages of bacterial outer membrane protein folding. *Cell*, 185, 1143–1156.
- Fairman, J.W., Dautin, N., Wojtowicz, D., Liu, W., Noinaj, N., Barnard, T.J. et al. (2012) Crystal structures of the outer membrane domain of intimin and invasins from enterohemorrhagic *E. coli* and enteropathogenic *Y. pseudotuberculosis*. *Structure*, 20, 1233–1243.
- Flynn, R.A., Pedram, K., Malaker, S.A., Batista, P.J., Smith, B.A.H., Johnson, A.G. et al. (2021) Small RNAs are modified with N-glycans and displayed on the surface of living cells. *Cell*, 184, 3109–3124.
- Frankel, G., Candy, D.C., Fabiani, E., Adu-Bobie, J., Gil, S., Novakova, M. et al. (1995) Molecular characterization of a carboxy-terminal eukaryotic-cell-binding domain of intimin from enteropathogenic *Escherichia coli*. *Infection and Immunity*, 63, 4323–4328.
- Gabius, H.J., Cudic, M., Diercks, T., Kaltner, H., Kopitz, J., Mayo, K.H. et al. (2021) What is the sugar code? *ChemBiochem*, 23, e202100327.
- Georgiou, G., Stathopoulos, C., Daugherty, P.S., Nayak, A.R., Iverson, B.L. & Curtiss, R.C., III. (1997) Display of heterologous proteins on the surface of microorganisms: from the screening of combinatorial libraries to live recombinant vaccines. *Nature Biotechnology*, 15, 29–34.
- Gunasinghe, S.D., Shiota, T., Stubenrauch, C.J., Schulze, K.E., Webb, C.T., Fulcher, A.J. et al. (2018) The WD40 protein BamB mediates coupling of BAM complexes into assembly precursors in the bacterial outer membrane. *Cell Reports*, 23, 2782–2794.
- Guvench, O., Mallajosyula, S.S., Raman, E.P., Hatcher, E., Vanommeslaeghe, K., Foster, T.J. et al. (2011) CHARMM additive all-atom force field for carbohydrate derivatives and its utility in polysaccharide and carbohydrate–protein modeling. *Journal of Chemical Theory and Computation*, 7, 3162–3180.
- Hu, D., Tateno, H. & Hirabayashi, J. (2015) Lectin engineering, a molecular evolutionary approach to expanding the lectin utilities. *Molecules*, 20, 7637–7656.
- Hussain, S., Peterson, J.H., Bernstein, H.D. & Trent, M.S. (2021) Reconstitution of bam complex-mediated assembly of a trimeric porin into proteoliposomes. *MBio*, 12, e0169621.
- Jaroszewicz, W., Morcinek-Orłowska, J., Pierzynowska, K., Gaffke, L. & Węgrzyn, G. (2022) Phage display and other peptide display technologies. *FEMS Microbiology Reviews*, 46, 1–25.
- Jensen, P.H., Weiligun, D., Matthiesen, F., McGuire, K.A., Shi, L. & Højrup, P. (2005) Characterization of the oligomer structure of recombinant human mannan-binding lectin. *The Journal of Biological Chemistry*, 280, 11043–11051.
- Jong, W.S.P., ten Hagen-Jongman, C.M., den Blaauwen, T., Jan Slotboom, D., Tame, J.R.H., Wickström, D. et al. (2007) Limited tolerance towards folded elements during secretion of the autotransporter Hbp. *Molecular Microbiology*, 63, 1524–1536.
- Kollman, P.A., Massova, I., Reyes, C., Kuhn, B., Huo, S., Chong, L. et al. (2000) Calculating structures and free energies of complex molecules: combining molecular mechanics and continuum models. *Accounts of Chemical Research*, 33, 889–897.
- Larsen, F., Madsen, H.O., Sim, R.B., Koch, C. & Garred, P. (2004) Disease-associated mutations in human mannose-binding lectin compromise oligomerization and activity of the final protein. *The Journal of Biological Chemistry*, 279, 21302–21311.
- Leo, J.C., Oberhettinger, P., Chaubey, M., Schütz, M., Kühner, D., Bertsche, U. et al. (2015) The Intimin periplasmic domain mediates dimerisation and binding to peptidoglycan. *Molecular Microbiology*, 95, 80–100.
- Leo, J.C., Oberhettinger, P., Yoshimoto, S., Udatha, D.B.R.K.G., Morth, J.P., Schütz, M. et al. (2016) Secretion of the Intimin passenger domain is driven by protein folding. *The Journal of Biological Chemistry*, 291, 20096–20112.

- Lepur, A., Salomonsson, E., Nilsson, U.J. & Leffler, H. (2012) Ligand induced galectin-3 protein self-association. *The Journal of Biological Chemistry*, 287, 21751–21756.
- Leyton, D.L., Sevastyanovich, Y.R., Browning, D.F., Rossiter, A.E., Wells, T.J., Fitzpatrick, R.E. et al. (2011) Size and conformation limits to secretion of disulfide-bonded loops in autotransporter proteins. *The Journal of Biological Chemistry*, 286, 42283–42291.
- Li, J., Li, B. & Liu, M. (2019) One-step synthesis of mannose-modified polyethyleneimine copolymer particles as fluorescent probes for the detection of *Escherichia coli*. *Sensors and Actuators B: Chemical*, 280, 171–176.
- Lin, B., Qing, X., Liao, J. & Zhuo, K. (2020) Role of protein glycosylation in host-pathogen interaction. *Cell*, 9, 1022.
- Luo, Y., Frey, E.A., Pfuetzner, R.A., Creagh, A.L., Knoechel, D.G., Haynes, C.A. et al. (2000) Crystal structure of enteropathogenic *Escherichia coli* intimin–receptor complex. *Nature*, 405, 1073–1077.
- Lupo, F., Ingersoll, M.A. & Pineda, M.A. (2021) The glycobiology of uropathogenic *E. coli* infection: the sweet and bitter role of sugars in urinary tract immunity. *Immunology*, 164, 3–14.
- Magalhães, A., Duarte, H.O. & Reis, C.A. (2021) The role of O-glycosylation in human disease. *Molecular Aspects of Medicine*, 79, 100964.
- Mahdavi, S.Z.B., Oroojalian, F., Eyvazi, S., Hejazi, M., Baradaran, B., Pouladi, N. et al. (2022) An overview on display systems (phage, bacterial, and yeast display) for production of anticancer antibodies; advantages and disadvantages. *International Journal of Biological Macromolecules*, 208, 421–442.
- McWilliams, B.D., Torres, A.G., Sperandio, V. & Hovde, C.J. (2014) Enterohemorrhagic *Escherichia coli* adhesins. *Microbiology Spectrum*, 2, 1–32.
- Meuskens, I., Saragliadis, A., Leo, J.C. & Linke, D. (2019) Type V secretion systems: an overview of passenger domain functions. *Frontiers in Microbiology*, 10, 1163.
- Miller, N.L., Clark, T., Raman, R. & Sasisekharan, R. (2021) Glycans in virus–host interactions: a structural perspective. *Frontiers in Molecular Biosciences*, 8, 666756.
- Munera, D., Palomino, C. & Fernández, L.Á. (2008) Specific residues in the N-terminal domain of FimH stimulate type 1 fimbriae assembly in *Escherichia coli* following the initial binding of the adhesin to FimD usher. *Molecular Microbiology*, 69, 911–925.
- Oberhettinger, P., Leo, J.C., Linke, D., Autenrieth, I.B. & Schütz, M.S. (2015) The inverse autotransporter intimin exports its passenger domain via a hairpin intermediate. *The Journal of Biological Chemistry*, 290, 1837–1849.
- Piñero-Lambea, C., Bodelón, G., Fernández-Periáñez, R., Cuesta, A.M., Álvarez-Vallina, L. & Fernández, L.Á. (2015) Programming controlled adhesion of *E. coli* to target surfaces, cells, and tumors with synthetic adhesins. *ACS Synthetic Biology*, 4, 463–473.
- Pinho, S.S. & Reis, C.A. (2015) Glycosylation in cancer: mechanisms and clinical implications. *Nature Reviews. Cancer*, 15, 540–555.
- Raposo, C.D., Canelas, A.B. & Barros, M.T. (2021) Human lectins, their carbohydrate affinities and where to find them. *Biomolecules*, 11, 188.
- Reily, C., Stewart, T.J., Renfrow, M.B. & Novak, J. (2019) Glycosylation in health and disease. *Nature Reviews. Nephrology*, 15, 346–366.
- Ryckaert, S., Callewaert, N., Jacobs, P.P., Dewaele, S., Dewerte, I. & Contreras, R. (2007) Fishing for lectins from diverse sequence libraries by yeast surface display – an exploratory study. *Glycobiology*, 18, 137–144.
- Salema, V. & Fernández, L.Á. (2017) *Escherichia coli* surface display for the selection of nanobodies. *Microbial Biotechnology*, 10, 1468–1484.
- Salema, V., Mañas, C., Cerdán, L., Piñero-Lambea, C., Marín, E., Roovers, R.C. et al. (2016) High affinity nanobodies against human epidermal growth factor receptor selected on cells by *E. coli* display. *MAbs*, 8, 1286–1301.
- Salema, V., Marín, E., Martínez-Arteaga, R., Ruano-Gallego, D., Fraile, S., Margolles, Y. et al. (2013) Selection of single domain antibodies from immune libraries displayed on the surface of *E. coli* cells with two β -domains of opposite topologies. *PLoS One*, 8, e75126.
- Salomonsson, E., Carlsson, M.C., Osla, V., Hendus-Altenburger, R., Kahl-Knutson, B., Öberg, C.T. et al. (2010) Mutational tuning of galectin-3 specificity and biological function. *The Journal of Biological Chemistry*, 285, 35079–35091.
- Saraboji, K., Håkansson, M., Genheden, S., Diehl, C., Qvist, J., Weininger, U. et al. (2011) The carbohydrate-binding site in galectin-3 is preorganized to recognize a sugarlike framework of oxygens: ultra-high-resolution structures and water dynamics. *The Biochemist*, 51, 296–306.
- Sartorius, R., D'Apice, L., Prisco, A. & De Berardinis, P. (2019) Arming filamentous bacteriophage, a nature-made nanoparticle, for new vaccine and immunotherapeutic strategies. *Pharmaceutics*, 11, 437.
- Schüchner, S., Behm, C., Mudrak, I. & Ogris, E. (2020) The Myc tag monoclonal antibody 9E10 displays highly variable epitope recognition dependent on neighboring sequence context. *Science Signaling*, 13, eaax9730.
- Sciacchitano, S., Lavra, L., Morgante, A., Ulivieri, A., Magi, F., De Francesco, G. et al. (2018) Galectin-3: one molecule for an alphabet of diseases, from A to Z. *International Journal of Molecular Sciences*, 19, 379.
- Seetharaman, J., Kanigsberg, A., Slaaby, R., Leffler, H., Barondes, S.H. & Rini, J.M. (1998) X-ray crystal structure of the human galectin-3 carbohydrate recognition domain at 2.1-Å resolution. *The Journal of Biological Chemistry*, 273, 13047–13052.
- Sheriff, S., Chang, C.Y. & Ezekowitz, R.A.B. (1994) Human mannose-binding protein carbohydrate recognition domain trimerizes through a triple α -helical coiled-coil. *Nature Structural Biology*, 1, 789–794.
- Sojitra, M., Sarkar, S., Maghera, J., Rodrigues, E., Carpenter, E.J., Seth, S. et al. (2021) Genetically encoded multivalent liquid glycan array displayed on M13 bacteriophage. *Nature Chemical Biology*, 17, 806–816.
- Srinivasan, J., Cheatham, T.E., Cieplak, P., Kollman, P.A. & Case, D.A. (1998) Continuum solvent studies of the stability of DNA, RNA, and phosphoramidate–DNA helices. *Journal of the American Chemical Society*, 120, 9401–9409.
- St-Pierre, Y., Hsieh, T.-J., Lin, H.-Y., Tu, Z., Huang, B.-S., Wu, S.-C. et al. (2015) Structural basis underlying the binding preference of human galectins-1, -3 and -7 for Gal β 1-3/4GlcNAc. *PLoS One*, 10, e0125946.
- Stravalaci, M., Pagani, I., Paraboschi, E.M., Pedotti, M., Doni, A., Scavello, F. et al. (2022) Recognition and inhibition of SARS-CoV-2 by humoral innate immunity pattern recognition molecules. *Nature Immunology*, 23, 275–286.
- Takahashi, K. & Ezekowitz, R.A.B. (2005) The role of the mannose-binding lectin in innate immunity. *Clinical Infectious Diseases*, 41, S440–S444.
- Talaga, M.L., Fan, N., Fueri, A.L., Brown, R.K., Bandyopadhyay, P. & Dam, T.K. (2016) Multitasking human lectin galectin-3 interacts with sulfated glycosaminoglycans and chondroitin sulfate proteoglycans. *The Biochemist*, 55, 4541–4551.
- Tomasek, D., Rawson, S., Lee, J., Wzorek, J.S., Harrison, S.C., Li, Z. et al. (2020) Structure of a nascent membrane protein as it folds on the BAM complex. *Nature*, 583, 473–478.
- Touzé, T., Hayward, R.D., Eswaran, J., Leong, J.M. & Koronakis, V. (2004) Self-association of EPEC intimin mediated by the β -barrel-containing anchor domain: a role in clustering of the Tir receptor. *Molecular Microbiology*, 51, 73–87.

- Valdés-Tresanco, M.S., Valdés-Tresanco, M.E., Valiente, P.A. & Moreno, E. (2021) gmx_MMPBSA: a new tool to perform end-state free energy calculations with GROMACS. *Journal of Chemical Theory and Computation*, 17, 6281–6291.
- Valldorf, B., Hinz, S.C., Russo, G., Pekar, L., Mohr, L., Klemm, J. et al. (2022) Antibody display technologies: selecting the cream of the crop. *Biological Chemistry*, 403, 455–477.
- van Ulsen, P., Rahman, S., Jong, W.S., Daleke-Schermerhorn, M.H. & Luirink, J. (2014) Type V secretion: from biogenesis to biotechnology. *Biochimica et Biophysica Acta – Molecular Cell Research*, 1843, 1592–1611.
- Vang Petersen, S. (2001) The mannan-binding lectin pathway of complement activation: biology and disease association. *Molecular Immunology*, 38, 133–149.
- Varki, A. (2017) Biological roles of glycans. *Glycobiology*, 27, 3–49.
- Wang, X., Peterson, J.H., Bernstein, H.D. & Trent, M.S. (2021) Bacterial outer membrane proteins are targeted to the bam complex by two parallel mechanisms. *MBio*, 12, e00597-21.
- Ward, E.M., Kizer, M.E. & Imperiali, B. (2021) Strategies and tactics for the development of selective glycan-binding proteins. *ACS Chemical Biology*, 16, 1795–1813.
- Warkentin, R. & Kwan, D.H. (2021) Resources and methods for engineering “designer” glycan-binding proteins. *Molecules*, 26, 380.
- Weikum, J., Kulakova, A., Tesei, G., Yoshimoto, S., Jægerum, L.V., Schütz, M. et al. (2020) The extracellular juncture domains in the intimin passenger adopt a constitutively extended conformation inducing restraints to its sphere of action. *Scientific Reports*, 10, 21249.
- Weis, W.I., Drickamer, K. & Hendrickson, W.A. (1992) Structure of a C-type mannose-binding protein complexed with an oligosaccharide. *Nature*, 360, 127–134.
- Wentzel, A., Christmann, A., Adams, T. & Kolmar, H. (2001) Display of passenger proteins on the surface of *Escherichia coli* K-12 by the enterohemorrhagic *E. coli* intimin EaeA. *Journal of Bacteriology*, 183, 7273–7284.
- Zelensky, A.N. & Gready, J.E. (2005) The C-type lectin-like domain superfamily. *The FEBS Journal*, 272, 6179–6217.
- Zhang, X.-L. & Qu, H. (2021) The role of glycosylation in infectious diseases. In: Lauc, G. & Trbojević-Akmačić, I. (Eds.) *The role of glycosylation in health and disease*, vol. 1325. Cham: Springer. https://doi.org/10.1007/978-3-030-70115-4_11

SUPPORTING INFORMATION

Additional supporting information can be found online in the Supporting Information section at the end of this article.

How to cite this article: Vázquez-Arias, A., Vázquez-Iglesias, L., Pérez-Juste, I., Pérez-Juste, J., Pastoriza-Santos, I. & Bodelon, G. (2024) Bacterial surface display of human lectins in *Escherichia coli*. *Microbial Biotechnology*, 17, e14409. Available from: <https://doi.org/10.1111/1751-7915.14409>